Influence of Nonlinear Rotor-Platform Interface on Dual-Spin Attitude Dynamics

Donald L. Cronin*
University of Missouri-Rolla, Rolla, Mo.

Atmosphere Explorer-C – a dual-spin spacecraft – exhibits a bounded attitude instability characterized most importantly by persistent coning of its spin axis about the intended direction of spin. Nonlinearities, presumably at the rotor-platform interface, were identified as the likely cause of the observed behavior. In the present paper, a rational nonlinear interface model is developed, and it is shown by integration of quasilinear equations of motion, and by approximate analysis, that the hypothesized model leads to behavior which predicts that observed.

Nomenclature

A = rotor transverse axis inertia
$\bar{A}$ = $A+\mu b'(b+b')$
$\boldsymbol{b}$ = $b\boldsymbol{n}_3$
$\boldsymbol{b}'$ = $b'\boldsymbol{n}_3'$
C = rotor spin axis inertia
c = coefficient of viscous friction
D = bearing ball diameter
d_m = bearing pitch diameter
I = $I_{33}C/\bar{I}_{33}$
$[I]$ = platform inertia matrix, $I_{ij}=0, i\neq j$
$[I']$ = rotor inertia matrix, $I_{ij}'=0, i\neq j$, tr $I'=A,A,C$
$\bar{I}_{ii}$ = $I_{ii}+A+\mu(b+b')^2, i=1,2$
$\bar{I}_{33}$ = $I_{33}+C$
$\tilde{I}_{ii}$ = $I_{ii}+\mu b(b+b'), i=1,2$
$\bar{I}_f$ = $\bar{I}_{11}=\bar{I}_{22}$, axisymmetric case
$\bar{I}_t$ = $\bar{I}_{11}=\bar{I}_{22}$, axisymmetric case
k_b = gain factor in motor control loop
k_f = gain factor in motor control loop
k_t = gain factor in motor control loop
m = mass of platform
m' = mass of rotor
r = $\bar{A}/\bar{I}_t$
r_i = $\bar{A}/\bar{I}_{ii}, i=1,2$
s = $\mu bb'/\bar{I}_t$
s_i = $\mu bb'/\bar{I}_{ii}, i=1,2$
$\boldsymbol{T}$ = $\Sigma T_i\boldsymbol{n}_i$
$\boldsymbol{u}$ = $\Sigma u_i\boldsymbol{n}_i$
$\boldsymbol{v}$ = $\Sigma v_i\boldsymbol{n}_i$
α = bearing contact angle
β = ring damper symmetry axis inertia
$\tilde{\beta}$ = $\beta/\bar{I}_{22}$
γ = ring damper coefficient of viscous friction
$\tilde{\gamma}$ = $\gamma/\bar{I}_{22}$
δ = decay rate; inverse of time of decay to $1/e$ of initial value
δ_r = decay rate for rigid system with ring damper
δ_s = decay rate for system
θ = cone angle, half cone angle
λ = $C\sigma_0/\bar{I}_t$
λ_i = $C\sigma_0/\bar{I}_{ii}, i=1,2$
μ = $mm'/(m+m')$
ρ = coefficient of Coulomb friction
τ_i = $T_i/\bar{I}_{ii}, i=1,2$
τ_f = time constant in motor control loop

Received March 15, 1976; revision received May 24, 1976. This study was performed while the author was a NASA-ASEE Summer Fellow at NASA Goddard Space Flight Center. Technical data and background material for this study were supplied by NASA and RCA personnel to whom the writer is indebted. The author acknowledges the help of H. Hoffman, Head of Goddard's Spacecraft Stabilization Branch; and T. Flatley of the same organization, who made available the results of his own investigations and critically reviewed the work reported here.

Index category: Spacecraft Attitude Dynamics and Control.

*Associate Professor, Department of Mechanical and Aerospace Engineering.

Introduction

ATMOSPHERE Explorer-C is theoretically stable in all of its operating modes. Its axisymmetric rotor portion is a large, fairly rigid momentum wheel supported by a single ball bearing and driven by redundant brushless dc motors. Its platform portion is an almost axisymmetric structure on which are mounted the spacecraft's passive viscous ring nutation dampers. Contrary to theoretical predictions, AE-C exhibits a bounded attitude instability. Disturbance-induced coning of its spin axis is observed either to grow for small initial cone angles, or to decay for larger initial cone angles until an intermediate equilibrium cone angle is reached. Steady precession of the spacecraft spin axis at this equilibrium angle follows. There exists, moreover, a threshold for this behavior, a very small cone angle below which induced coning motion appears to decay more or less normally.

Investigations led to an identification of the rotor-platform interface as the likely source of this attitude instability. The rotor-platform interface, it may be recalled, was previously identified as the source of the attitude instability of another dual-spin spacecraft, Tascat I.[1] Published work[2,3] concerning the influence of interface parameters on dual-spin attitude dynamics employs linear interface models and predicts no stability dependence on cone angle. Nonspecifically located nonlinear stiffness and dissipation mechanisms were shown,[4,5] on the other hand, to be capable of causing a

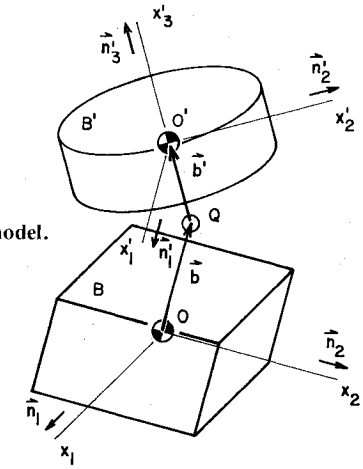

Fig. 1 Idealized spacecraft model.

variety of attitude behaviors including the steady precession previously described.

In the present paper, the flexible, dissipative interface of a dual-spin spacecraft is characterized generally in terms of documented nonlinearities: hardening stiffness of the bearing connecting the spacecraft portions, and Coulomb friction proportional to bearing stiffness.[6] Included also are viscous terms intended to describe the influence of bearing lubricant, and terms describing the influence of motors employed to preserve relative spin. A nutation damper is also present. Quasi-linear equations of motion are derived, and an approximate analysis is developed. The quasi-linear and approximate descriptions of the hypothesized model are employed to examine the specific case of AE-C functioning with its platform despun, one of two normal operating modes. These descriptions are shown to predict the observed AE-C attitude instability.

Equations of Motion

The system analyzed is illustrated schematically in Fig. 1. The axisymmetric rotor B' spins about its center line contiguous to the vector b' drawn from the point of rotor-platform connection Q to $0'$, the rotor's center of mass. The platform B spins about an axis of symmetry contiguous to the vector b drawn from 0, the platform's center of mass, to Q.

Primed and unprimed coordinate systems are fixed in B' and B, respectively and originate at mass centers as shown. Associated unit vectors are related through the semilinearized transformation

$$\{n'\}=[U]\{n\}$$

$$U=\begin{bmatrix} c & s & a_1 \\ -s & c & a_2 \\ \phi_2 & -\phi_1 & 1 \end{bmatrix} \tag{1}$$

with

$$c=\cos\phi_3,\quad s=\sin\phi_3,\quad a_1=-\phi_2 c+\phi_1 s,\quad a_2=\phi_2 s+\phi_1 c$$

Small angles ϕ_1 and ϕ_2 illustrated in Fig. 2 characterize, to first order, rotations of B' with respect to B about orthogonal axes normal to the system axis of spin; ϕ_3 characterizes relative rotor spin.

Equations of motion given by Cretcher and Mingori[7] may be restated, for the systems

$$[I]\dot{u}+u\times([I]u)+[I']\dot{v}+v\times([I']v)$$
$$+\mu(b+b')\times(\ddot{b}+\ddot{b}')=0 \tag{2}$$

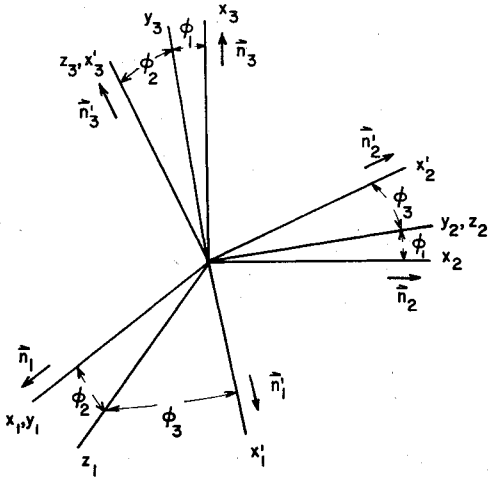

Fig. 2 Orientation of coordinate systems.

and for the platform

$$[I]\dot{u}+u\times([I]u)+\mu b\times(\ddot{b}+\ddot{b}')=T \tag{3}$$

Dots over vectors signify total differentation with respect to time. Primed and unprimed inertia quantities are developed about primed and unprimed axes, respectively.

Components of Eqs. (2) and (3) along the x_1, x_2, and x_3 axes may be written with the aid of the transformation in Eq. (1). Subject to the assumptions of small transverse platform rates u_1 and u_2, and small interface angular deflections ϕ_1 and ϕ_2, component equations accurate to first order in small quantities are

$$\begin{aligned}
&\bar{I}_{11}\dot{u}_1+(\bar{I}_{33}-\bar{I}_{22})u_2u_{30}+C\sigma_0u_2\\
&+[C(u_{30}+\sigma_0)-2\bar{A}u_{30}]\dot{\phi}_2\\
&+[(C-\bar{A})u_{30}+C\sigma_0]u_{30}\phi_1+\bar{A}\ddot{\phi}_1=0\\
&\bar{I}_{22}\dot{u}_2-(\bar{I}_{33}-\bar{I}_{11})u_1u_{30}-C\sigma_0u_1\\
&-[C(u_{30}+\sigma_0)-2\bar{A}u_{30}]\dot{\phi}_1\\
&+[(C-\bar{A})u_{30}+C\sigma_0]u_{30}\phi_2+\bar{A}\ddot{\phi}_2=0\\
&\bar{I}_{33}\dot{u}_{31}+C\dot{\sigma}_1=0
\end{aligned} \tag{4a}$$

for the spacecraft, and

$$\begin{aligned}
&\bar{I}_{11}\dot{u}_1+(I_{33}-\bar{I}_{22})u_2u_{30}+\mu bb'(\ddot{\phi}_1-u_{30}^2\phi_1)\\
&-2\mu bb'u_{30}\dot{\phi}_2=T_1\\
&\bar{I}_{22}\dot{u}_2-(I_{33}-\bar{I}_{11})u_1u_{30}+\mu bb'(\ddot{\phi}_2-u_{30}^2\phi_2)\\
&+2\mu bb'u_{30}\dot{\phi}_1=T_2\\
&I_{33}\dot{u}_{31}=T_3
\end{aligned} \tag{4b}$$

for the platform, with

$$u_3=u_{30}+u_{31},\quad u_{30}\gg u_{31},\quad \dot{u}_{30}=0$$
$$\dot{\phi}_3=\sigma_0+\sigma_1,\quad \sigma_0\gg\sigma_1,\quad \dot{\sigma}_0=0$$

Torques transmitted across the rotor-platform interface may be attributed to a motor (or motors), a bearing (or bearings), and to miscellaneous connections such as seals and slip rings assemblies. AE-C employs two motors in tandem (either normally operates), and a single X-contact or four-point contact ball bearing interposed between the motors. Miscellaneous connections include an encoder assembly and two labyrinth seals.

An estimate for bearing torque employs the model illustrated in Fig. 3. The inner portion of the bearing – rotor mounted inner race, retainer, and balls – is treated as a single disk-like body constrained against rotation about axes in a plane bisecting the bearing and parallel to the x_1, x_2 plane by an elastic housing representing the platform-mounted outer race.

To first order, the instantaneous axis of disk relative transverse rotation is parallel to the unit vector n_r

$$n_r=(\phi_1 n_1+\phi_2 n_2)/\phi$$

$$\phi=(\phi_1^2+\phi_2^2)^{1/2}$$

Contact of the disk and housing is centered in a plane containing the x_3 axis and normal to n_r. The pressure of the disk on the housing produces a net normal force

$$F_s=f(\phi)n_\alpha$$

with

$$\boldsymbol{n}_\alpha = \cos\alpha \boldsymbol{n}_f + \sin\alpha \boldsymbol{n}_3$$

$$\boldsymbol{n}_f = (-\phi_2 \boldsymbol{n}_1 + \phi_1 \boldsymbol{n}_2)/\phi$$

This force is generally a nonlinear function of deflection; it is treated here, however, as a first-order quantity. Contact angle dependence on applied loading is relatively weak for an X-contact bearing. Changes in α, the contact angle, are considered here, therefore, to be first-order quantities. Their influence on $\boldsymbol{F}_s$ is thus negligible.

The moment arm associated with $\boldsymbol{F}_s$ requires definition only to zero order

$$\boldsymbol{R} = \tfrac{1}{2}[(d_m + D\cos\alpha)\boldsymbol{n}_f + D\sin\alpha \boldsymbol{n}_3]$$

The torque produces by $\boldsymbol{F}_s$ and its counterpart on the opposite side of the bearing is

$$\begin{aligned}\boldsymbol{T}_s &= 2\boldsymbol{R} \times \boldsymbol{F}_s \\ &= d_m \sin\alpha f(\phi)\boldsymbol{n}_r \\ &= M(\phi)\boldsymbol{n}_r \end{aligned} \tag{5}$$

Contact force is assumed to include a Coulomb term

$$\boldsymbol{G} = -\mathrm{sgn}(\sigma_0)\rho f(\phi)\boldsymbol{n}_r$$

The force $\boldsymbol{G}$ is again a first-order quantity requiring for description its direction only to zeroth order. The associated torque is

$$\boldsymbol{T}_c = 2\boldsymbol{R} \times \boldsymbol{G}$$

$$\boldsymbol{T}_c = -\mathrm{sgn}(\sigma_0)\rho f(\phi)[D\sin\alpha \boldsymbol{n}_f - (d_m + D\cos\alpha)\boldsymbol{n}_3] \tag{6}$$

$$\boldsymbol{T}_c = -\bar{\rho} M(\phi)[\boldsymbol{n}_f - (d_m + D\cos\alpha)/D\sin\alpha \boldsymbol{n}_3]$$

with

$$\bar{\rho} = \mathrm{sgn}(\sigma_0) D\rho/d_m$$

To torques given in Eqs. (5) and (6) is added a viscous torque serving to characterize bearing lubricant dissipation mechanisms

$$\boldsymbol{T}_v = \boldsymbol{T}_{vo} + \boldsymbol{T}_{vI}$$

$$\boldsymbol{T}_{vo} = c\sigma_0 \boldsymbol{n}_3 \tag{7a}$$

$$\boldsymbol{T}_{vI} = c(\dot{\phi}_1 \boldsymbol{n}_1 + \dot{\phi}_2 \boldsymbol{n}_2 + \sigma_1 \boldsymbol{n}_3) \tag{7b}$$

Motor drive torque is assumed parallel to the skewed rotor centerline. Components of drive torque applied to the platform are then

$$\boldsymbol{T}_M = \boldsymbol{T}_{Mo} + \boldsymbol{T}_{MI}$$

$$\boldsymbol{T}_{M0} = -c\sigma_0 \boldsymbol{n}_3 \tag{8a}$$

$$\boldsymbol{T}_{MI} = -T_{MI}(\phi_2 \boldsymbol{n}_1 - \phi_1 \boldsymbol{n}_2 + \boldsymbol{n}_3)$$

The constant viscous torque term given in Eq. (7a) is faithfully reacted by the constant motor torque term given in Eq. (8a).

The spacecraft attitude behavior described in the introduction appears in all modes of motor control including the simplest, a tachometer speed control, described in Fig. 4 and characterized for present purposes by

$$I\dot{\sigma}_1 = T_{MI} - \boldsymbol{n}_3 \cdot (\boldsymbol{T}_c + \boldsymbol{T}_{vI}) \tag{9a}$$

$$\tau_f \dot{T}_{MI} + T_{MI} = -k_b k_t \tau_f \dot{\sigma}_1 - (k_b k_t + k_f k_a k_t)\sigma_1 \tag{9b}$$

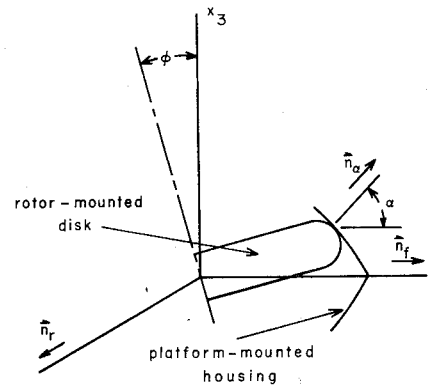

Fig. 3 Idealized bearing model.

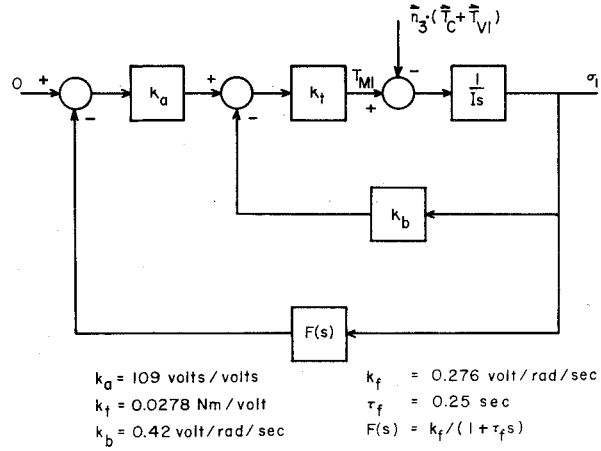

Fig. 4 Tachometer speed control incorporating AE parameters.

Disturbance torques appearing on the right-hand side of Eq. (9a) are first-order. Time-dependent motor torque T_{MI} is first order for properly designed control. Transverse components of time-dependent motor torque shown in Eq. (8b) are second order and are, therefore, negligible.

Motor rotors are displaced from the bearing-bisecting plane of transverse rotation. Rotation of the rotor assembly about an axis in this plane parallel to $\boldsymbol{n}_r$ produces a translation of motor rotors and a disruption of motor air gap symmetry leading to additional platform torques in the $-\boldsymbol{n}_r$ and $-\mathrm{sgn}(\sigma_0)\boldsymbol{n}_f$ directions (as well as a ϕ dependent component along the rotor center line). These torques are presently uncharacterized, as are presumed small torques associated with the encoder assembly and labyrinth seals.

Consistent with the foregoing order-of-magnitude arguments, spacecraft behavior may be described to first-order accuracy by the first two of Eqs. (4a) and the first two of Eqs. (4b). In the latter

$$T_i = \boldsymbol{n}_i \cdot (\boldsymbol{T}_s + \boldsymbol{T}_c + \boldsymbol{T}_{vI}),\ i = 1,2 \tag{10}$$

where expressions for $\boldsymbol{T}_s, \boldsymbol{T}_c$, and $\boldsymbol{T}_{vI}$ are given in Eqs. (5), (6), and (7b), respectively.

Further work is simplified by the assumption of negligible platform spin, i.e., $u_{30} = 0$. In this case, equations of motion may be written

$$\begin{aligned} \dot{u}_1 + \lambda_1(u_2 + \dot{\phi}_2) + r_1\ddot{\phi}_1 &= 0 \\ \dot{u}_2 - \lambda_2(u_1 + \dot{\phi}_1) + r_2\ddot{\phi}_2 &= 0 \\ \dot{u}_1 + s_1\ddot{\phi}_1 &= \tau_1 \\ \dot{u}_2 + s_2\ddot{\phi}_2 &= \tau_2 \end{aligned} \tag{11a}$$

Platform mounted viscous-ring nutation dampers having centerlines along the x_2 axis contribute the following terms to the left-hand side of Eqs. (11a).

$$\begin{Bmatrix} 0 \\ \tilde{\beta}\dot{\omega} \\ 0 \\ -\tilde{\gamma}\omega \end{Bmatrix} \tag{11b}$$

and add the equation

$$\beta(\dot{\omega}+\dot{u}_2)+\gamma\omega=0 \tag{11c}$$

where

$$\omega=\omega n_2$$

describes the damper fluid rotation rate.

Results of numerically integrating Eqs. (11a) with addition (11b), and Eq. (11c) are given and discussed in a subsequent section.

Approximation

An approximation may be developed for the case of an axisymmetric spacecraft. Given axisymmetry

$$\tilde{I}_{11}=\tilde{I}_{22}=\tilde{I}_t, \quad \tilde{I}_{11}=\tilde{I}_{22}=\tilde{I}_t$$

in Eqs. (4a) and (4b), and

$$\lambda_1=\lambda_2=\lambda$$

$$r_1=r_2=r$$

$$s_1=s_2=s$$

in Eqs. (11a).

Interface torques discussed previously may be summarized

$$\begin{aligned} \tau_1 &= [c\dot{\phi}_1+M(\phi)(\phi_1+\tilde{\rho}\phi_2)/\phi]/\tilde{I}_t \\ \tau_2 &= [c\dot{\phi}_2+M(\phi)(\phi_2-\tilde{\rho}\phi_1)/\phi]/\tilde{I}_t \end{aligned} \tag{12}$$

In Eqs. (11a), the substitutions

$$u_{12}=u_1+ju_2$$

$$\phi_{12}=\phi_1+j\phi_2$$

and manipulation give

$$\begin{aligned} \dot{u}_{12}-j\lambda u_{12}+r\ddot{\phi}_{12}-j\lambda\phi_{12}&=0 \\ \dot{u}_{12}+s\ddot{\phi}_{12}&=j\tilde{c}\dot{\phi}_{12}+\tilde{M}(\phi)(1-j\tilde{\rho})\phi_{12} \end{aligned} \tag{13}$$

with

$$\tilde{c}=c/\tilde{I}_t, \quad \tilde{M}(\phi)=M(\phi)/(\tilde{I}_t\phi)$$

In Eq. (13), the assumed solutions

$$u_{12}=Ue^{pt}$$

$$\phi_{12}=\Phi e^{pt}$$

lead to relationships

$$U=-p(rp-j\lambda)\Phi/(p-j\lambda) \tag{14}$$

and

$$Q(p)-(p-j\lambda)[\tilde{c}p-j\tilde{\rho}\tilde{M}(\phi)]/(r-s)=0 \tag{15}$$

and

$$Q(p)=-p^3-jd_2p^2+d_1p+jd_0$$

where

$$d_2=-\lambda(1-s)/(r-s)$$

$$d_1=-\tilde{M}(\phi)/(r-s)$$

$$d_0=\lambda\tilde{M}(\phi)/(r-s)$$

and

$$1>r>s$$

for the present study. In Eq. (15) $\tilde{M}(\phi)$ is treated as an average over one coning cycle.

The roots of the polynomial given in Eq. (15) depend upon the spacecraft cone angle θ through the interface torque $M(\phi)$, since the time rate of change of rotor angular momentum equals the applied torque

$$M(\phi)\doteq C\sigma_0\lambda\theta \tag{16}$$

One root solving Eq. (15) is generally near $j\lambda$, where λ is the rigid body precession frequency. The real part of this root, therefore, describes coning growth or decay. The case of marginal stability may be examined by assuming a solution to Eq. (15) of the form

$$p=jm$$

with m real. Substitution reveals two requirements on m

$$\tilde{c}m-\tilde{\rho}\tilde{M}(\phi)=0 \tag{17a}$$

and

$$m^3+d_2m^2+d_1m+d_0=0 \tag{17b}$$

The three solutions to Eq. (17b) are sketched in Fig. 5 as functions of $\tilde{M}(\phi)$. The straight line described by Eq. (17a) intersects two of the solution curves; the lower intersection provides the marginally stable flexible precession frequency m_1^*, and the corresponding interface torque $\tilde{M}^*(\phi)$. The latter may be employed in Eq. (16) to approximate the marginally stable cone angle. (In Eq. (16) m_1^* replaces λ to more accurately reflect the situation.)

The mode shape associated with marginally stable precession may be obtained from Eq. (14)

$$\begin{Bmatrix} U \\ \\ \phi \end{Bmatrix} \approx \begin{Bmatrix} 1 \\ \\ \dfrac{j(\lambda-m_1^*)}{m_1^*(\lambda-rm_1^*)} \end{Bmatrix}$$

with

$$\lambda>m_1^*>rm_1^*$$

Deflection at the interface is seen to lead coning by 90°. More significant is that Coulomb torque, which is seen to lag deflection in Eqs. (13) by 90°, is in phase with transverse rate (and platform angular momentum); it is therefore destabilizing. Viscous torque, on the other hand, leads deflection by 90°, and is thus 180° out of phase with platform angular momentum; it is therefore stabilizing.

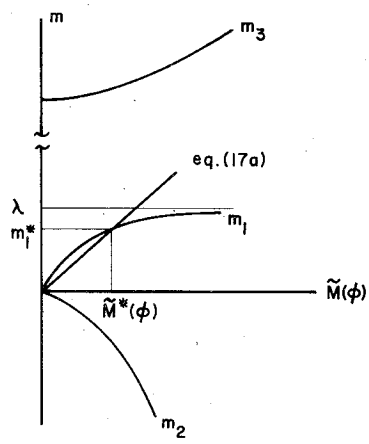

Fig. 5 Sketch of m vs $\tilde{M}(\phi)$ behavior for Eqs. (17a) and (17b).

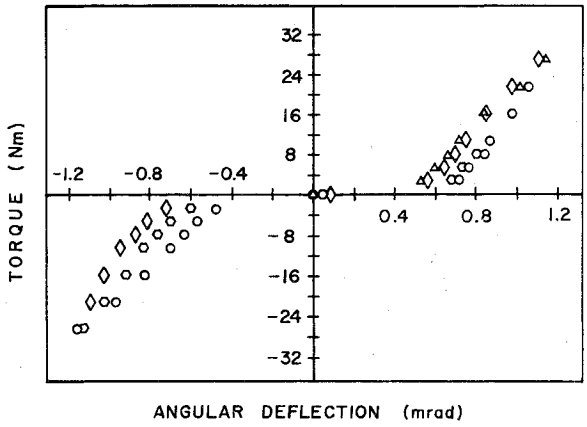

Fig. 6 Experimental torque-angular deflection data for spacecraft bearing (source: T. Flatley, NASA).

Coulomb torque increases relative to viscous torque for increased interface deflection, since the bearing typically exhibits hardening stiffness. Both $M(\phi)$ and $\tilde{M}(\phi)$ are thus monotonically increasing functions of ϕ (and cone angle). The spacecraft is thus unstable for cone angles larger than the marginally stable cone angle, and stable for smaller cone angles. The marginally stable cone angle described here is therefore the threshold cone angle characterizing spacecraft behavior.

Stability may be investigated in further detail by assuming a solution to Eq. (15) of the form

$$p = jm_1 + p_1$$

with $m_1 \gg |p_1|$. Use of a truncated Taylor series for $Q(p)$

$$Q(p) \doteq Q(jm_1) + p_1 Q'(jm_1) \doteq p_1 Q'(jm_1)$$

with

$$Q'(jm_1) = 3m_1^2 + 2d_2 m_1 + d_1$$

leads to an expression for p_1

$$p_1 = (\lambda - m_1)[\bar{c}m_1 - \bar{\rho}\tilde{M}(\phi)]\{Q'(jm_1)(r-s) + j[\bar{c}(2m_1 - \lambda) - \bar{\rho}\tilde{M}(\phi)]\}/\Delta$$

with

$$\Delta = [Q'(jm_1)(r-s)]^2 + [\bar{c}(2m_1 - \lambda) - \bar{\rho}\tilde{M}(\phi)]^2$$

Coning growth or decay is described by $Re(p_1)$

$$\delta = (\lambda - m_1)[\bar{c}m_1 - \bar{\rho}\tilde{M}(\phi)]Q'(jm_1)(r-s)/\Delta \qquad (18)$$

and the flexible precession frequency is given by $m_1 + Im(p_1)$. In Eq. (18)

$$\Delta > 0$$

$$(\lambda - m_1) > 0$$

$$(r-s) > 0$$

$$Q'(jm_1) < 0$$

Stable behavior, that is, coning decay, therefore requires that

$$\bar{c}m_1 - \bar{\rho}\tilde{M}(\phi) > 0 \qquad (19)$$

Above the threshold angle, the interface effects described here are seen to always destabilize. It is shown in the next section, however, that this destabilization is strong only over a fairly narrow range of spacecraft cone angle and becomes less significant as cone angle increases. System decay rate δ_s is also controlled by the viscous ring nutation dampers. For the system

$$\delta_s = \delta + \delta_r$$

where δ is obtained from Eq. (18), and where δ_r is the decay rate of the rigid spacecraft with the ring dampers. The equilibrium cone angle characterizing spacecraft behavior is thus possible with the model developed here. It occurs when the destabilizing influence of interface effects is balanced by the stabilizing influence of the viscous ring dampers.

The approximation given in this section represents a potentially useful approach for assessing the influence of other interface effects, both linear and nonlinear. Assume, for example, that motor torque was nonnegligible and that one desired its inclusion. To the right-hand side of Eqs. (12) is added

$$\begin{Bmatrix} -\tau_{M1}\phi_2 \\ \tau_{M1}\phi_1 \end{Bmatrix}$$

where

$$\tau_{M1} = T_{M1}/\tilde{I}_t$$

This produces in the second of Eqs. (13) the new right-hand term

$$j\tau_{M1}\phi_{12}$$

For perfect motor control

$$\tau_{M1} = \bar{\rho}M(\phi)(d_m + D\cos\alpha)/D\sin\alpha/\tilde{I}_t > 0 \qquad (20)$$

from Eq. (6) when $\text{sgn}(\sigma_0) > 0$. Motor torque is 180° out of phase with platform angular momentum and serves to stabilize. Marginal spacecraft stability obtains where the line

$$\bar{c}m + \tau_{M1} - \bar{\rho}\tilde{M}(\phi) = 0 \qquad (21)$$

intersects the m_1 curve in Fig. 5. A stability requirement becomes

$$\bar{c}m_1 + \tau_{M1} - \bar{\rho}\tilde{M}(\phi) > 0$$

The m axis intercept of Eq. (20) is negative. An intersection with the m_2 curve therefore occurs, indicating a second

Table 1 AE-C properties

Quantity	Value	Units
m	751.97	kg
m'	13.32	kg
b	44.2	cm
b'	9.6	cm
$\bar{I}_{11}$	117.12	kg m^2
$\bar{I}_{22}$	118.88	kg m^2
$\bar{I}_{33}$	136.63	kg m^2
A	1.80	kg m^2
C	3.59	kg m^2
β	1.75	kg m^2
γ	0.32	Nm sec/rad
σ_0	37.70	rad/sec

marginally stable cone angle. One may repeat the steps given above proceeding from Eq. (15) and an assumed solution

$$p = jm_2 + p_2$$

where $-m_2 \gg |p_2|$ to obtain another stability criterion

$$\tilde{c}m_2 + \tau_{M1} - \tilde{\rho}\tilde{M}(\phi) < 0$$

since it may be shown that

$$Q'(jm_2) > 0$$

Discussion of Results

Cone angle growth for AE-C is observed for cone angles in the range 0.05° to 0.75°. Similar instability is exhibited by the model described above when AE-C properties are employed and when interface dissipation parameters c and ρ are suitably adjusted. Appropriate properties are listed in Table 1. Values shown for the nutation dampers provide a 12 min coning decay time constant for the rigid spacecraft.

Static torque-angular deflection data for an installed bearing are shown in Fig. 6. Several analytical descriptions for these data were employed during the study. The simplest

$$M(\phi) = 1.0445 \times 10^{10}\phi^3 Nm \qquad (22)$$

with ϕ measured in radians, was most often utilized.

For values quoted in Table 1, integration of Eqs. (11a) with addition (11b), and Eq. (11c) produced results typified by the time constant-cone angle plot shown in Fig. 7. In this plot are seen, in addition to the range of coning growth, the stabilizing influence of interface dissipation below the threshold cone angle, and the asymptotic approach of time constant to the rigid spacecraft value in the range above the equilibrium cone angle.

Integration established that essential behavior was significantly influenced neither by starting values specified for interface deflections and rates, nor by the analytical description for $M(\phi)$ – piecewise linear and fifth-order representations were used in addition to the cubic given in Eq. (22). Motor and control were included, adding Eqs. (9) and modifying Eq. (10); this inclusion again produced no significant change in essential behavior.

At this point the strongest admissible conclusions are that the interface is the source of the observed instability and that nonlinear bearing stiffness is the direct or indirect cause. Dissipative interface torques employed here either associate with bearing dissipation mechanisms as presumed in the development, or they associate with unspecified mechanisms, and the words linking them to the bearing are gratuitous. To associate these torques more or less positively with the bearing, one must establish that the values for interface dissipation parameters needed to match model behavior to spacecraft behavior can be justified by comparison to the results of bearing test or analysis.

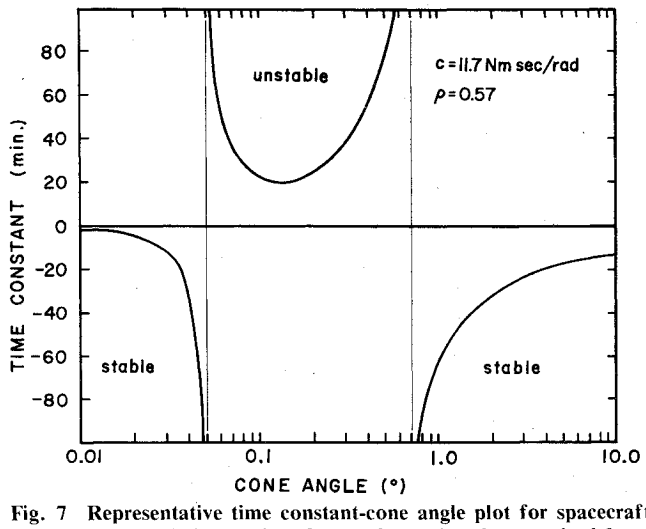

Fig. 7 Representative time constant-cone angle plot for spacecraft with nonlinear, dissipative interface and nutation damper sized for a nominal 12 min coning decay time constant.

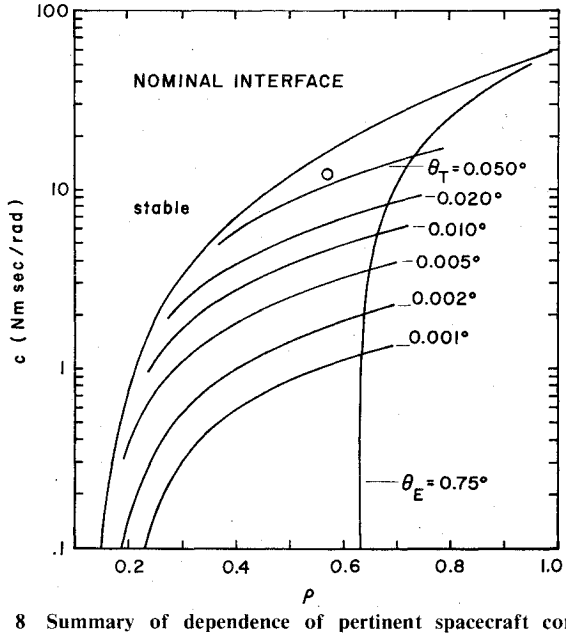

Fig. 8 Summary of dependence of pertinent spacecraft coning behavior on interface dissipation parameters for the nominally stiff interface.

The situation is complicated by several uncertainties. First, data shown for bearing torque vs angular deflection may not be representative, since this behavior depends critically on individual bearing internal dimensions and upon temperature. Second, the threshold angle is not precisely known. The value quoted is believed to be an upper bound.

Figures 8, 9, and 10 are intended to give a concise summary of spacecraft coning dependence on interface dissipation parameters. Employed in the construction of these figures were Eqs. (18) and (20). The leftmost curve on each figure represents the boundary above which values of c and ρ permit stable operation. Below the leftmost curve various unstable behavior is possible. Unstable behavior characterized, for example, by an equilibrium cone angle θ_E of 0.75°, is produced by values of c and ρ lying on the rightmost curve of each figure. Values of c and ρ on a member curve of the families shown produce unstable behavior characterized by the label threshold cone angle θ_T. The nominally stiff interface referred to on Fig. 8 is defined by Eq. (22). Softer and stiffer interfaces are defined, respectively, as those producing half or twice the nominal torque at an interface deflection of 0.46 mrad.

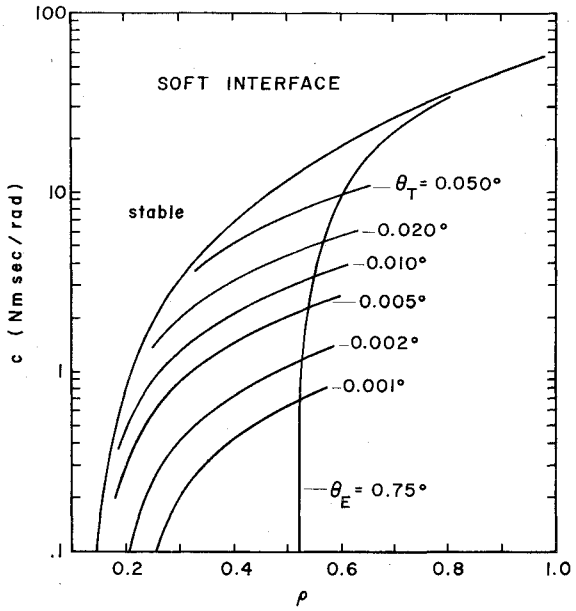

Fig. 9 Summary of dependence of pertinent spacecraft coning behavior on interface dissipation parameters for the softer than nominal interface.

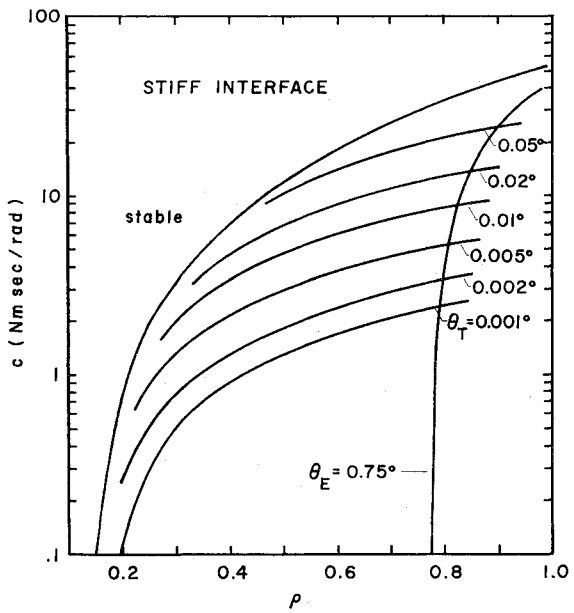

Fig. 10 Summary of dependence of pertinent spacecraft coning behavior on interface dissipation parameters for the stiffer than nominal interface.

Values of c and ρ employed to generate Fig. 7 are indicated by the circle on Fig. 8. Approximate analysis is seen to accurately predict threshold cone angle, and to fall short in the prediction of equilibrium cone angle. Intersections shown on Figs. 8-10 serve to establish, within the context of uncertainties described, ranges within which c and ρ must lie to cause the observed spacecraft behavior. Admissible values for ρ, hypothesized to describe bearing Coulomb friction, do lie within the order-of-magnitude range of published bearing values, 0.06-0.07[8].

Bearing work does not generally employ the simple viscous friction model. Admissible values for the viscous friction coefficient c are believed, however, to be generally higher than values one could reasonably attribute to the bearing. One is left to conclude that if the associated torque employed here is indeed caused by bearing dissipation mechanisms, then the interface is considerably softer than Fig. 6 data suggest and/or the threshold cone angle is considerably lower than 0.05°.

Conclusion

Two distinct features are employed in the present rotor-platform interface model. One, Coulomb friction, is considered representative of bearing dissipative behavior and has been shown, by implication, to always destabilize a dual-spin spacecraft. The other, nonlinear bearing stiffness, causes instability to depend on cone angle.

The destabilizing influence of interface Coulomb friction as modified by nonlinear bearing stiffness could have been countered in the case of AE-C – if the results shown in Fig. 7 are representative – by a nutation damper sized to provide a rigid spacecraft coning decay time constant of less than 7.5 min.

The launches of AE-D and AE-E took place after this study was completed. Atmosphere Explorer-D cones at an equilibrium angle of 1° in the platform despun mode and does not exhibit a detectable threshold. The latter behavior reinforces the suggestion that the AE-C threshold may be considerably lower than formerly thought. Early attitude instability of AE-E disappeared after the activation of a new augmenting platform-mounted nutation damper. The theoretical or rigid spacecraft coning decay time constant for AE-E is considerably less than 7.5 min.

An improved understanding of dual spin rotor-platform interface behavior should lead for future programs to appropriate specification of requisite nutation damping, and possibly, to new self-stabilizing interface designs. It is hoped that the present work enhances understanding and suggests directions for related analytical and experimental studies.

References

[1] Johnson, C. R., "TACSAT I Nutation Dynamics," AIAA Paper 70-455, Los Angeles, Calif., 1970.

[2] Scher, M. P., "Effects of Flexibility in the Bearing Assemblies of Dual-Spin Spacecraft," *AIAA Journal*, Vol. 9, May 1971, pp. 900-905.

[3] Willems, P. Y., "Effect of Bearing Flexibility on Dual-Spin Satellite Attitude Stability," *Journal of Spacecraft and Rockets*, Vol. 9, August 1972, pp. 587-591.

[4] Mingori, D. L., Tseng, G. T. and Likins, P. W., "Constant and Variable Limit Cycles in Dual-Spin Spacecraft," *Journal of Spacecraft and Rockets*, Vol. 9, Nov. 1972, pp. 825-830.

[5] Likins, P. W., Tseng, G. T. and Mingori, D. L., "Stable Limit Cycle Due to Nonlinear Damping in Dual-Spin Spacecraft," *Journal of Spacecraft and Rockets*, Vol. 8, June 1971, pp. 568-574.

[6] Jones, A. B., "Ball Motion and Sliding Friction in Ball Bearings," Trans. ASME, *Journal of Basic Engineering*, Vol. 81, March 1959, pp. 1-12.

[7] Cretcher, C. K. and Mingori, D. L., "Nutation Damping and Vibration Isolation in a Flexibly Coupled Dual-Spin Spacecraft," *Journal of Spacecraft and Rockets*, Vol. 8, August 1971, pp. 817-823.

[8] Jones, A. B., "Ball Motion and Sliding Friction in Ball Bearings," Trans. ASME, *Journal of Basic Engineering*, March 1959, p. 12.